GESEP – Gerência de Especialistas em Sistemas Elétricos de Potência

Título:

LCL filter losses due to harmonic compensation in a photovoltaic system.

Autores:

G. L. E. Mata, R. C. de Barros, W. V. Ribeiro, L. S. Xavier, A. F. Cupertino and H. A. Pereira.

Publicado em:

8th International Symposium on Power Electronics for Distributed Generation Systems (PEDG)

Data da publicação:

2017

Citação para a versão publicada:

G. L. E. Mata, R. C. de Barros, W. V. Ribeiro, L. S. Xavier, A. F. Cupertino and H. A. Pereira, "LCL filter losses due to harmonic compensation in a photovoltaic system," 2017 IEEE 8th International Symposium on Power Electronics for Distributed Generation Systems (PEDG), Florianopolis, 2017, pp. 1-7.

LCL Filter Losses due to Harmonic Compensation in a Photovoltaic System

Guilherme L. E. Mata[1], Rodrigo C. de Barros[1], Wesley V. Ribeiro[1], Lucas S. Xavier[1,3], Allan F. Cupertino[1,2], Heverton A. Pereira[1].

[1]Gerência Especialistas em Sistemas Elétricos de Potência
Universidade Federal de Viçosa
Av. P. H. Rolfs s/nº, 36570-000
Viçosa, MG, Brazil
rodrigocdebarros@gmail.com,
wv.ribeiro92@hotmail.com, glevangelista48@gmail.com,
heverton.pereira@ufv.br

[2]Centro Federal de Educação Tecnológica de Minas Gerais
Av. Amazonas 5253, 30421-169
Belo Horizonte, Brazil
allan.cupertino@yahoo.com.br

[3]Graduate Program in Electrical Engineering
Federal University of Minas Gerais
Av. Antônio Carlos 6627, 31270-901
Belo Horizonte, MG, Brazil
lsantx@gmail.com

Abstract — **Nowadays, non-linear loads are one of the major issues regarding the system power quality. Additionally, the growing presence of distributed generation (DG) systems, which employs converters to connect power sources to the grid may also affect power quality due to its switching. To better utilize such converters, multifunctional operation is usually employed. In order to reduce the harmonics generated by the switching, passive filters interface converter connection to the grid and any loads as well. This work performs an analysis of how the multifunctional operation of the photovoltaic inverter, specifically during harmonic current compensation, affects the efficiency of the system. Therefore, the power losses of the LCL filter are analyzed.**

I. Introduction

As the energy demand increases over the world, the use of alternative energy sources is increasing, especially the photovoltaic (PV) generation. PV modules and inverters prices have declined in the last years, also installations costs declined in increased speed in some economies, which lead to a total cost reduction of around 75% in less then 10 years [1]. Also, DG systems have change the traditional infrastructure conception of electrical power systems, consisting in the installation of small and medium-sized plants near the consumer units, utilizing mostly renewable energy sources. This type of installation is attracting more attention due to the growth of the environmental concerns about energy generation [1].

To perform the connection of the PV plant to the grid, its necessary to utilize electronic converters. Fig. 1 presents a diagram of a single phase grid-connected PV system. These converters may affect negatively the power quality in the grid due to the injection of harmonic currents into the power system [2]. In addition, non-linear load connected to the point of common coupling (PCC) also degrade the power quality in the grid [3].

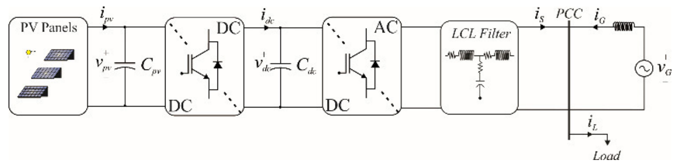

Fig. 1. Single-phase grid-connected photovoltaic system.

The LCL filter is the most used structure to reduce harmonics generated due to inverter switching [4]. Despite a LCL filter to be a simple passive structure, special attention is necessary in its design. The filter must be modeled in order that the losses are not high enough to reduce the converter efficiency [5].

Usually, the main function of a photovoltaic inverter is to inject active power into the grid. Nevertheless, as solar irradiance varies during the day, the converter works below its nominal operation point, presenting a margin to perform some ancillary services that help the power quality improvement [6]. One of these ancillary services is harmonic current compensation present in the non-linear load connected to the system [3]. As some standards establish that the total harmonic distortion level of a system must be below 5% [7]. Thus, performing an ancillary service is an economic viable alternative than using active or passive filters.

978-1-5090-5339-1/17/$31.00

This work performs an analysis of the power losses in the LCL filter to determine if utilizing the multifunctional operation of the PV inverter for harmonic current compensation reduces converter efficiency. The study considered only the ohmic losses in the damping resistance and the resistance associated with the filter inductors.

The methodology for harmonic detection and control of the current components being compensated are described in section II. Then, in section III, the utilized LCL filter modeling methodology is described. After, section IV presents three case studies that are analyzed in section V, where the obtained results through simulation are discussed. Finally conclusions are stated in Section VI.

II. METHODOLOGY

The modeling of the main elements of the studied grid-connected system are presented below.

A. Photovoltaic Panels Model

In this work, the PV panels are modeled as described in [8]. This mathematical approximation is based on the characteristic curve of voltage by current from the PV panels. The resistances represent the voltage drop and losses for both current going to the load (R_s) and the reverse leakage current of the diode (R_p), respectively. The model is presented in Fig. 2.

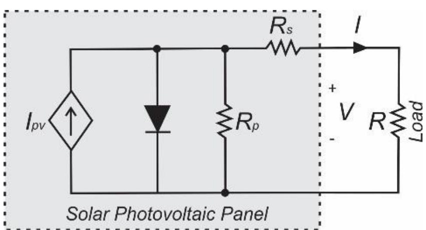

Fig. 2. Model of a solar photovoltaic panel.

B. Control strategy

The systems control strategy used in this work is shown in Fig. 3. Fig. 3(a) presents the dc/dc stage block diagram. This stage is responsible to extract the maximum power from the PV plant and to ensure that voltage on the inverter dc bus does not vary, granting stability. The outer loop of this stage controls the voltage on the PV modules dc-bus, v_{pv}, and tracks the maximum power point of them, utilizing the Incremental Conductance method [9]. The inner loop controls boost inductor current I_{ind}^{*}.

The inverter control block diagram is shown in Fig. 3(b). The outer loop of this stage is based on the energy stored in the bus capacitor, given by (1). The time derivative of this relation gives the instantaneous capacitor power, p_{cp}. Thus, the power injected by the inverter can be written as:

$$W = \frac{1}{2} C_{dc} v_{dc}^{2}, \tag{1}$$

$$p_{inv} = p_{pv} + p_{cap}. \tag{2}$$

Thus, the relation between p_{cap} and v_{pv} is expressed by

$$v_{pv}^{2} = \frac{p_{cap}}{2C_{dc}s}. \tag{3}$$

Considering that the current inner loop is ideal, the outer closed-loop transfer function, G_{out} ,is obtained:

$$G_{out} = \frac{v_{pv}^{2}}{v_{pv}^{*2}} = \frac{2k_p(\tau_i s + 2)}{\tau_i C_{dc} s^2 + 2k_p(\tau_i s + 2)}, \tag{4}$$

where k_p and τ_i are the PI controller parameters. The controller is tuned through the pole allocation method, in order to ensure a low overshoot response.

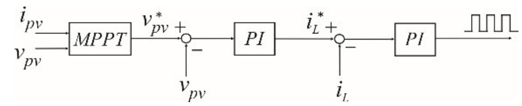

(a)

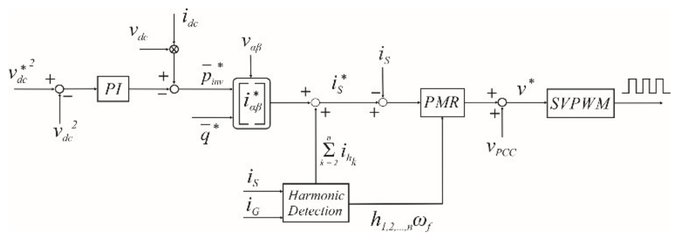

(b)

Fig. 3 Control diagrams of the photovoltaic system: (a) Boost converter block diagram. (b) Inverter block diagram.

The model of current control is derived as follows. Disregarding the effects of the capacitor in the LCL filter, the inverter dynamic in αβ stationary coordinates is given by:

$$v_\alpha - Ri_\alpha - L\frac{di_\alpha}{dt} - V_\alpha = 0, \tag{5}$$

$$v_\beta - Ri_\beta - L\frac{di_\beta}{dt} - V_\beta = 0, \tag{6}$$

where v_α and v_β are the voltages on the inverter side of the filter, L and R are the sum of the inductances L_g and L_f, and the sum of the resistances R_g and R_f respectively, i_α and i_β are the inverter current on the αβ reference frame, and V_α and V_β are the voltages measured in the PCC.

The active current is obtained from the Instantaneous Power Theory [3] and can be written as in (7). In this study, no reactive power is injected. Summing this current with the harmonic current from the detection method gives the inverter reference current:

$$i^{*}(t) = 2\frac{\bar{p}_{inv}^{*} v_\alpha + v_\beta \bar{q}^{*}}{V_\alpha + V_\beta}. \tag{7}$$

Proportional multi-resonant controllers (PMR) are used to control the sinusoidal currents. As the detection method is adaptive and able to detect harmonic components of any frequency in the load, utilizing PR controllers tuned in the detected frequency simplify the control strategy and makes it more precise, since proportional integral (PI) controllers present steady state errors due to their limited bandwidth. One resonant controller is necessary for each component of the signal, thus one for the fundamental component and one for each harmonic component being compensated. It can be expressed in the s-domain as:

$$G(s) = K_p^R + \sum_h K_{i,h}^R \frac{s}{s^2 + \omega_h^2}. \quad (8)$$

where K_p^R is the proportional gain and $K_{i,h}^R$ is the resonant gain. The last term of (8) is responsible for tracking the harmonics at ω_h frequency. The harmonic detector dynamically adjusts these frequencies, while the gains are adjusted according to [10], in order to mitigate instabilities that can occur if harmonics are above the crossover frequency of the controller loop.

C. Harmonic Detector

The harmonic detection method is detailed in [11] and can be seen in Fig. 4. It bases on the interaction between the second order generalized integrator (SOGI) adaptive filter, connected in cascade with a synchronous reference frame phase-locked loop (SRF-PLL). The SOGI detects the harmonic in the frequency fed by the PLL, and the PLL extracts the amplitude, frequency and phase of the harmonic component.

Associating more SOGI-PLL structures in cascade allows to detect as many components as desired. The first structure detects the fundamental load current component, while the others detect the harmonic components in order of predominance: the highest amplitude harmonic component is detected by the second structure, the second highest by the third structure, etc.

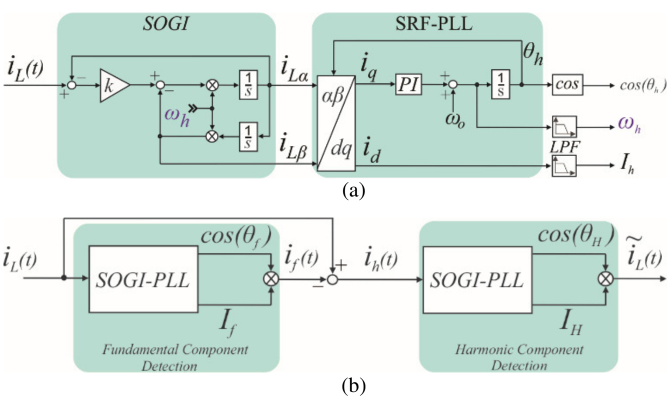

Fig. 4. Current component detection method. (a) SOGI-PLL structure. (b) Cascade SOGI-PLL for multiple harmonic detection.

III. LCL Filter Modeling

The LCL filter design is based on the methodology proposed by [12]. The filter inductances and capacitance are calculated as function of the total harmonic distortion (THD), the power factor and voltage drop. Firstly, the following parameters need to be defined: Rated power of the converter S_n, grid voltage V_n, grid frequency f_n, the dc-link voltage V_{dc} and the swithing frequency f_{sw}. Three ratios are employed in the filter design: the ratio between f_{sw} and the filter resonant frequency f_{res}, called r_f, the ratio between the filter inductances, called $r_l = L/L_g$ and ratio between the per unit values of the filter equivalent inductance and the filter capacitance, called r_q.

The ratio r_f ratio is important in terms of stability of the control system and it affects directly the performance of active damping approaches. In this work, $r_f \approx 3$ is adopted, as suggested by [12].

The total inductance of the filter in p.u. is given by (9):

$$l_T = r_f \cdot \frac{f_n}{f_{sw}} \cdot \frac{1 + r_l}{\sqrt{r_l \cdot r_q}}. \quad (9)$$

When $r_l = 1$, the minimum inductance values and minimum voltage drop across the filter is obtained. Additionally, equal inductances are economically advantageous. For this reason, $r_l = 1$ is employed in this work and $L = L_g$.

Furthermore, the output current THD of the LCL filter at the nominal operating point can be approximated by [12]:

$$THD = \frac{100}{I_n} \frac{\pi\, v_{dc}}{12\, Z_b} \frac{\sqrt{r_q}}{r_f^3} \frac{\sqrt{r_L}}{1 + r_L} \frac{1}{\left(1 - \frac{6}{m_f}\right)^2 - \frac{1}{r_f^2}} \sqrt{f(m)}, \quad (10)$$

where $m_f = f_{sw}/f_n$ and:

$$m = \frac{\sqrt{3}}{V_{dc}} \sqrt{\frac{V_n^2}{3} + (\omega_n L_T I_n)^2}, \quad (11)$$

$$f(m) = \frac{3}{2}m^2 - \frac{4\sqrt{3}}{\pi} + \frac{9}{8}\left(\frac{3}{2} - \frac{9}{8}\frac{\sqrt{3}}{\pi} m^4\right), \quad (12)$$

Finally, the filter power factor can be estimated by:

$$PF = 1 - \frac{q^2}{2}, \quad (13)$$

where

$$q = \frac{r_q - 1}{\sqrt{r_q}} \frac{1 + \mathrm{r_l}}{\sqrt{r_l}} \mathrm{r_f} \frac{\mathrm{f_n}}{\mathrm{f_{sw}}}. \quad (14)$$

If $r_q = 1$, the filter power factor is unitary. However, this choose results in low capacitance values and high inductances. Generally r_q is changed in order to reduce the inductance values to acceptable values. Finally, the filter parameters are calculated by:

$$C_f = r_q \cdot \frac{L_T}{Z_b^2}, \quad (15)$$

$$L_f = \frac{L_T}{r_l + 1}, \quad (16)$$

$$L_g = r_l \cdot L_f, \tag{17}$$

$$f_{res} = \frac{1}{2\cdot\pi}\cdot\sqrt{\frac{1}{C_f}\cdot\left(\frac{1}{L_f}+\frac{1}{L_g}\right)}. \tag{18}$$

where $L_T = l_T\, L_b$, $L_b = Z_b/\omega_n$ and $Z_b = S_n/V_n^2$.

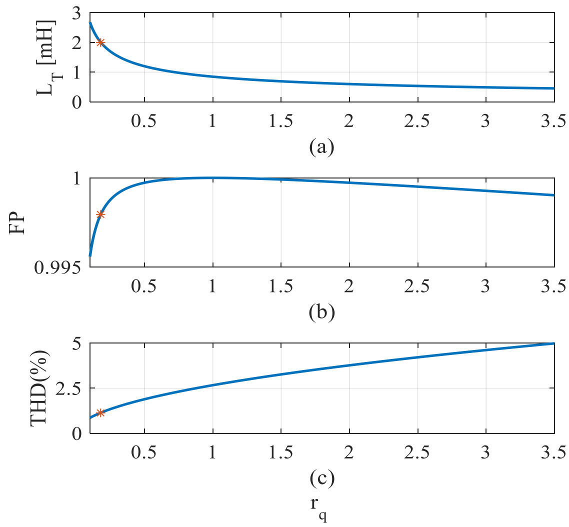

Fig. 5. Design of LCL filter: (a) Effect of r_q in the filter total inductance; (b) Effect of r_q in the filter power fator; (c) Effect of r_q in the output current THD.

Considering $S_n = 5\,kVA$, $V_{dc} = 390\,V$, $V_n = 220\,V$ and $f_{sw} = 12\,kHz$, the per unit inductance value l_t, the THD and the power factor PF is plotted as function of r_q, as shown in Fig. 5 order to obtain relatively small inductances with acceptable values of PF and THD, $r_q = 0.18$ is employed. This choose results in a power factor larger than 0.995 and a THD smaller than 2 %.

The damping resistance is calculated in order to reduce the filter resonance. However, it interferes in the control stability. Thus, taking in consideration both of these conditions and the inductances and capacitances already chosen, a root locus diagram for the closed loop system is built. The R_d value is chosen analyzing the damping factor of the filter and stability in such diagram [12].

IV. Case Study

This work proposes an analysis of a 5 kW single-phase PV system. The array was composed of 2 strings in parallel with 10 PV panels of 250 W connected in series in each one, resulting in the power specified. The characteristics of the PV panel utilized are listed in Table I. System parameters and controller gains can be found in Table II and Table III, while the harmonic detector parameters are in Table IV. In all simulations, there is a linear load that consumes 5 kW. The non-linear load utilized is simulated through sinusoidal current controlled sources. All simulations were implemented in PLECS environment.

To the first case study, various simulations are performed in order to obtain the LCL filter losses when the inverter performs only harmonic current compensation. Irradiance is set to zero, therefore no active current is injected by the inverter. Just one harmonic current was being compensated and its harmonic order and the current amplitudes are varied. Two PR controllers are used: one adjusted to the fundamental frequency of the grid and the other dynamically tuned on the load harmonic component frequency being compensated.

The load used in this case study is composed of a linear load that consumes 5 kW and a non-linear load with one harmonic component. Initially, the load is composed of a 5th order harmonic component with amplitude of 2 A and the losses for this configuration are obtained. After that, the amplitude is changed to 5 A, after to 10 A and finally 15 A. The same process is made for the 7th, 11th and 13th harmonics.

The second case study focuses on showing the losses behavior during active power injection with harmonic compensation. The irradiance is changed to 500 W/m^2, thus the inverter injects half of its rated current (16 A), and the non-linear load has one harmonic component of the 5th order with 10 A. In this situation, two PR controllers are also employed.

In the third case study, a harmonic component of the 7th order is added to the previous case, with amplitude of 5 A. Therefore, three PR controllers are utilized.

TABLE I. PV Panel Parameters

Variable	Description	Value
P_n	Nominal Power (W)	250
V_{ocn}	Open Circuit Nominal Voltage (V)	35.5
I_{scn}	Short Circuit Nominal Current (A)	8.5
V_{mp}	Maximum Power Point Voltage (V)	31.29
I_{mp}	Maximum Power Point Current (A)	7.99

TABLE II. Simulation Parameters

Variable	Description	Value
f_{sw}	Switching frequency (kHz)	12
f_{sa}	Sampling frequency (kHz)	12
f_n	Grid frequency (Hz)	60
V_{PCC}	PCC Voltage (V)	220
V_{dc}	DC link Voltage (V)	390
C_{bus}	DC bus capacitance (µF)	500
C_f	LCL filter capacitance (µf)	3.8
L_f, L_g	LCL filter inductances (mH)	1
R_f, R_g	LCL filter resistance associated to the inductors L_f, L_g (mΩ)	19
R_d	LCL filter damping resistance (Ω)	4

TABLE III. CONTROLERS GAINS

Variable	Description	Value
K_{p-sdc}	Prop. Gain of dc bus voltage loop	0.3770
K_{i-sdc}	Integral Gain of dc bus voltage loop	3.9478
K_{p-res}	Prop. Gain of PMR	14.833
K_{i-res}	Integral Gain of PMR	2000
K_{p-VL}	Prop. Gain of boost converter voltage loop	1.508
K_{i-VL}	Integral Gain of boost converter voltage loop	158.733
K_{p-IL}	Prop. Gain of boost converter current loop	0.193
K_{i-IL}	Integral Gain of boost converter current loop	0.387

TABLE IV. HARMONIC DETECTOR PARAMETERS

Description	Value
SOGI-PLL Parameters of the 1st Stage	$k = 0.8$ $\xi = 0.707$ $\omega_n = 6\pi$
SOGI-PLL Parameters of the 2nd and 3rd Stages	$k = 0.8$ $\xi = 0.707$ $\omega_n = 60\pi$

TABLE V. POWER LOSSES DUE TO ACTIVE POWER INJECTION.

	5 A	10 A	16 A	32 A
$\boldsymbol{R_d}$	4.1 W	4.07 W	4.05 W	3.91 W
$\boldsymbol{R_f}$	0.22 W	0.86 W	2.34 W	9.64 W
$\boldsymbol{R_g}$	0.2 W	0.88 W	2.32 W	9.63 W
Total	4.53 W	5.81 W	8.71 W	23.18 W

The data is collected from 3 elements in the filter: the damping resistance R_d, and the resistance associated with the filter inductors, one on the inverter side, R_f, and the other on the grid side, R_g. Inductors magnetic losses and capacitor losses are not evaluated in this work.

V. SIMULATION RESULTS

To provide a mean of comparison, the power losses due to only active power injection can be found in Table V. Note that the R_d losses do not vary much around 4 W, while the R_f and R_g losses increase significantly with the amplitude.

A. First Case

The results for the first case, with only one harmonic component compensation, are presented in Fig. 6. The damping resistor losses, are shown in Fig. 6(a), and are the predominant ones. The losses in the filter inductors are less significant, as seen in Fig. 6(b) e Fig. 6(c), being representative only for high amplitudes.

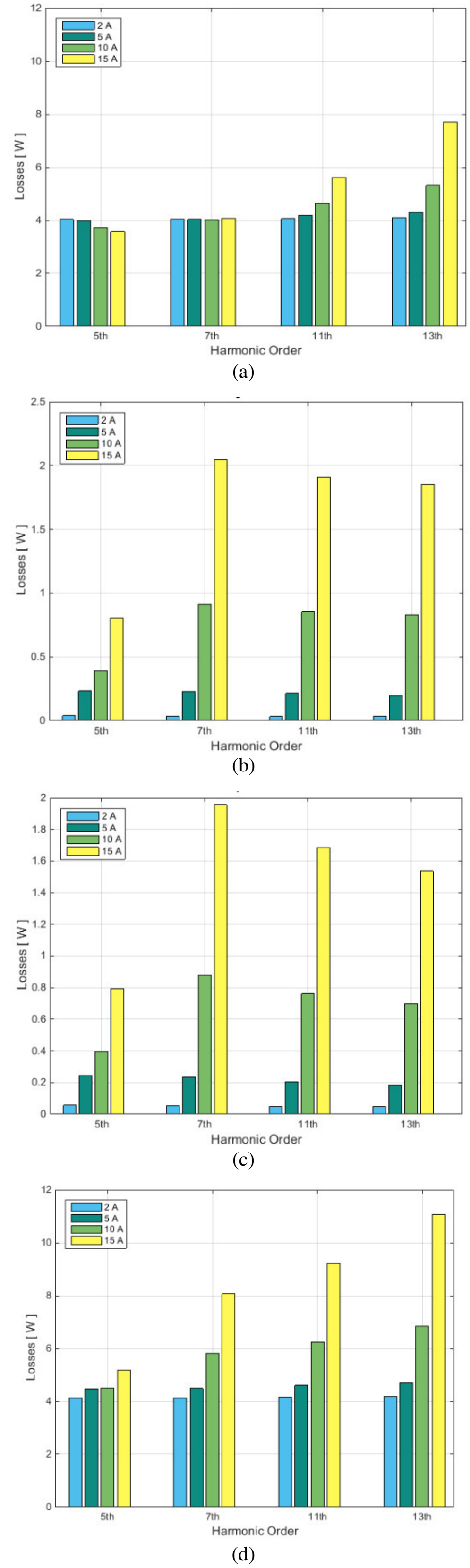

Fig. 6. LCL filter losses for the 5th, 7th, 11th and 13th harmonics. (a) $\boldsymbol{R_d}$ Losses. (b) $\boldsymbol{R_g}$ Losses. (c) $\boldsymbol{R_f}$ Losses. (d) Total Losses.

The harmonic losses have a similar behavior for low frequencies, but for high frequencies the R_d losses increase with the amplitude, while the R_f and R_g are lower than the losses for low frequencies. This occurs due to the current interaction with the filter inductors, generating an induced voltage that might not be in phase with the inverter voltage or PCC voltage, causing such discrepancy.

Therefore, the total losses presented in Fig. 6(d), are mainly due to the damping resistance. For higher amplitudes, the inductors losses have larger contribution, but the damping resistor losses still contribute more for the total.

In Fig. 7, a 3D view of the total losses in p.u. is presented. The behavior of the losses associated with 5^{th} and 7^{th} harmonics are almost linear, while for the 11^{th} and 13^{th} harmonics there is notable increase.

B. *Second Case*

Fig. 8 shows the filter losses when the inverter injects 16 A of active current and 10 A of 5^{th} harmonic current. Comparing with Fig. 6 for this harmonic order, the presence of the active current increases significantly the losses in the inductor resistances. Note that the damping resistor losses are around 4 W, as observed during only active power injection and for low frequency harmonic compensation.

C. *Third Case*

With the injection of two harmonics, from 5^{th} order with 10 A and 7^{th} order with 5 A, together with 16 A of active current, the filter losses are presented in Fig. 9. These result are very similar to those obtained in the previous case, with the R_f and R_g losses being slightly higher.

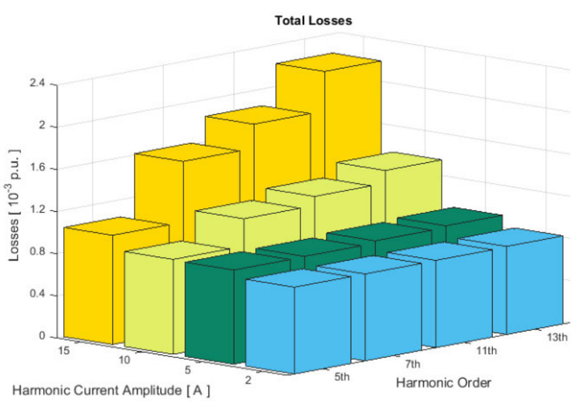

Fig. 7. LCL filter losses as function of the harmonic order and amplitude.

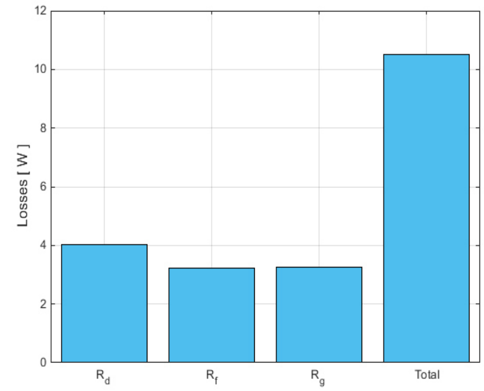

Fig. 8. Filter losses during fundamental and 5^{th} harmonic component current injection.

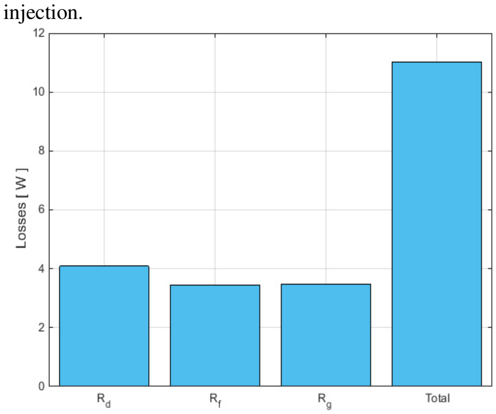

Fig. 9. Filter losses during fundamental, 5^{th} and 7^{th} harmonic current component injection.

VI. CONCLUSIONS

This work analyzes the losses on the LCL filter of a grid connected PV system. The three cases presented explored different combinations of fundamental and harmonic current being injected by the inverter. The studies also showed that, as expected, the losses increase with the current amplitude and the frequency, presenting a significant difference to the 5^{th} for the 13^{th} harmonic order.

However, it is possible to observe that in all cases such losses were not greater then 15 W, in a system of 5 kW. Table VI and Table VII presents the percentage losses for the cases studied. Note that for the worst case, with active current and two harmonic component injection, the losses are lower than 0.25%. of the rated power. Therefore, utilizing the inverter to realize this ancillary service does not compromise its efficiency.

TABLE VI. PERCENTAGE OF LOSSES IN RELATION TO THE INVERTER POWER

	2 A	5 A	10 A	15 A	16 A	32 A
Fund.	-	-	-	-	0.174	0.464
5^{th}	0.082	0.09	0.089	0.104	-	-
7^{th}	0.083	0.09	0.116	0.161	-	-
11^{th}	0.083	0.092	0.125	0.184	-	-
13^{th}	0.084	0.094	0.137	0.222	-	-

TABLE VII. PERCENTAGE OF LOSSES IN RELATION TO THE INVERTER POWER

	Fund. (A)	5^{th} (A)	7^{th} (A)	Total Losses (%)
Case II	16	10	-	0.21
Case III	16	10	5	0.221

Future studies of the inverter efficiency during harmonic current compensation may include an analysis of the switching losses, as well as the conduction losses.

ACKNOWLEDGMENT

The authors would like to thank to CNPQ, FAPEMIG and CAPES for their assistance and financial support.

REFERENCES

[1] M. Rekinger, F. Thies, G. Masson e S. Orlandi, Global Market Output For Solar Power / 2015-2019, SolarPower Europe, 2014.

[2] D. I. Brandão, F. P. Marafão, H. M. K. Paredes e A. Costabeber, Inverter control strategy for DG systems based on the Conservative Power Theory, IEEE Energy Conversio Congress and Exposition, pp. 3283-3290, 2013.

[3] J. He, Y. W. Li, F. Blaabjerg e X. Wang, Active Harmonic Filtering Using Current-Controlled, Grid-Connected DG Units With Closed-Loop Power Control, IEEE TRansaction on Power Electronics, pp. 2642-653, 2014.

[4] M. Liserre, F. Blaabjerg e S. Hansen, Design and control of an LCL-filter-based three-phase active rectifier, IEEE TRansactions on Industry Applications, vol. 41, pp. 1281-1291, 2005.

[5] V. Kaura e V. Blasko, Operation of a phase locked loop system inder distorted utility conditions, IEEE Transactions on Industry Applications, vol. 33, pp. 58-63, 1997.

[6] J. P. Bonaldo e J. A. Pomilio, Multi-functional use of single-phase power converters, IEEE PES Conference on Innovative Smart Grid Technologies Latin America (ISGT LA), pp. 1-6, 2013.

[7] IEEE, IEEE Standard for Interconnecting Distributed Resources with Electric Power Systems, 2003.

[8] M. G. Villalva, J. R. Gazoli e E. R. Filho, Comprehensive Approach to Modeling and Simulation of Photovoltaic Arrays, IEEE Transaction on Power Electronics, vol. 24, nº 1, pp. 1198-1208, 2009.

[9] D. Sera, L. Mathe, T. Kerekes, S. V. Sparatu e R. Teodorescu, On the Perturb-and-Observe and Incremental Conductance MPPT Methods for PV Systems, IEEE Journal of Photovoltaics, vol. 3, pp. 1070-1078, 2013.

[10] A. G. Yepes, F. D. Feijedo, O. Lopez e J. Dobal-Gandoy, Analysis and Design of Resonant Current Controllers for Voltage-Source Converters by Means of Nyquist Diagrams and Sensitivity Function, IEEE Transactions on Industrial Electronics, vol. 58, pp. 5231-5250, 2011.

[11] L. S. Xavier, A. F. Cupertino, J. T. d. Resende, V. F. Mendes e H. A. Pereira, Adaptive current control strategy for harmonic compensation in single-phase solar inverters., Electronic Power System Research, vol. 142, pp. 84-95, 2017.

[12] R. Peña-Alzola, M. Liserre, F. Blaabjerg e M. Ordonez, LCL-Filter Design for Robust Active Damping in Grid-Connected Converters, IEEE Transactions on Industrial Informatics, p. 2192, 2014.